Zircon composition as a fertility indicator of Archean granites

by

Y-J Lu, RH Smithies, MTD Wingate, NJ Evans[1], PA Morris, DC Champion[2] and TC McCuaig[3,4]

Porphyry Cu deposits are major sources of Cu and Mo. They range in age from Archean to modern, although most are Jurassic and younger, and porphyry deposits in Precambrian terranes are rare. Nevertheless, several porphyry-type Cu or Au deposits occur in the Superior Craton of Canada (Fayol and Jebrak, 2017), and in the South West Terrane of the Yilgarn Craton (McCuaig et al., 2001; Outhwaite, 2018), suggesting that their potential in Archean cratons may not be fully recognized. Chemical fingerprinting and assessment of potential targets from terrane to deposit scale are needed by industry (e.g. Ballard et al., 2002; Loucks, 2014; McCuaig and Hronsky, 2014; Agnew, 2015; Lu et al., 2016).

In Phanerozoic porphyry Cu systems, mineralized magmatic rocks have distinctive chemical compositions, including high Sr/Y, V/Sc, Eu/Eu*, and (Eu/Eu*)/Y ratios (e.g. Chiaradia et al., 2012; Loucks, 2014; Lu et al., 2017). Zircons in these rocks also have distinctive compositions, such as higher Eu/Eu* ratios (Ballard et al., 2002; Lu et al., 2016). These signatures can be attributed to high magmatic water and sulfur contents, and high oxidation states, and can be used as ore fertility indicators.

Archean granites in the Yilgarn Craton

To test whether these fertility indicators can be applied to Archean granites across the Yilgarn Craton, we have compiled Geological Survey of Western Australia (GSWA) geochronology and geochemistry data for 230 unaltered and non-mineralized granites. The granites are divided into four groups (Fig. 1), based on their K_2O/Na_2O and Sr/Y ratios:

- **potassic high Sr/Y granites** have $K_2O/Na_2O \geq 1$ and $Sr/Y \geq 40$
- **sodic high Sr/Y granites** have $K_2O/Na_2O < 1$ and $Sr/Y \geq 40$
- **sodic low Sr/Y granites** have $K_2O/Na_2O < 1$ and $Sr/Y < 40$
- **potassic low Sr/Y granites** have $K_2O/Na_2O \geq 1$ and $Sr/Y < 40$.

A K_2O/Na_2O ratio of 1 separates potassic and sodic groups. A Sr/Y ratio of 40 is used to distinguish between high and low Sr/Y groups because porphyry Cu deposits are associated with granites that have $Sr/Y \geq 40$ (Chiaradia et al., 2012; Loucks, 2014), and average Archean tonalite–trondhjemite–granodiorite (TTG) has Sr/Y >40 (Moyen and Martin, 2012). We also examined >2000 trace element analyses for zircons from 42 Yilgarn granite samples, although screening out alteration and mineral inclusions leaves 220 analyses from 30 samples (Fig. 1).

Fertility of Yilgarn granites revealed by whole-rock geochemistry

We compared Yilgarn granites with well-characterized hydrous and oxidized Miocene Cu-mineralized granites associated with porphyry Cu mineralization in the Lhasa Terrane of southern Tibet (Lu et al., 2015). The Tibetan granites crystallized from very hydrous magmas with >10 wt% water contents at depth, resulting mainly from high-pressure differentiation of hydrous mafic melts of sub-Tibetan mantle (Lu et al., 2015).

Figure 2a shows that neither hydrous melting nor dehydration melting of mafic lower crust can produce melts with Mg# >50. Tibetan granites typically have Mg# >50, some of which plot within the high-Mg diorite (HMD) field at 55–65 wt% SiO_2 (Fig. 2a), consistent with input of primary mafic magmas through magma mixing. In contrast, most Yilgarn granites have Mg# <50, suggesting derivation mainly through crustal melting with limited mantle input. This interpretation is supported by the observation that few mafic microgranular enclaves (MME, mantle-derived melts) are present in Yilgarn granites, whereas MME are common in Tibetan Cu-mineralized granites.

Based on Fe_2O_3/FeO ratios, Yilgarn high Sr/Y granites are moderately to strongly oxidized, whereas low Sr/Y granites are moderately reduced to strongly oxidized (Fig. 2b). Tibetan Cu-mineralized granites are mainly strongly oxidized and tend to have higher Fe_2O_3/FeO

1 John de Laeter Centre and Department of Applied Geology, Curtin University, Bentley, WA 6845, Australia

2 Geoscience Australia, GPO Box 378, Canberra, ACT 2601, Australia

3 BHP, 125 St Georges Terrace, Perth, WA 6000, Australia

4 Centre for Exploration Targeting and ARC Centre of Excellence for Core to Crust Fluid Systems, School of Earth Sciences, The University of Western Australia, Crawley, WA 6009, Australia

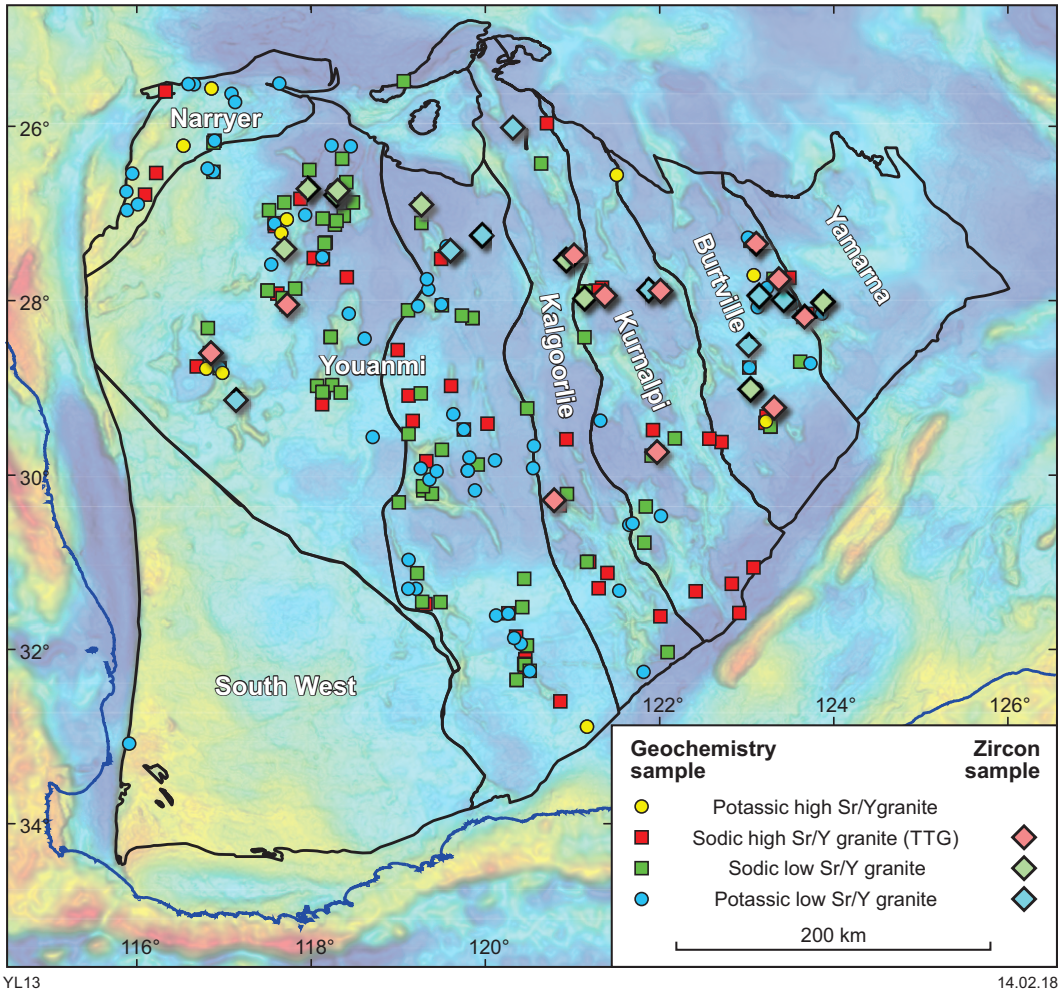

Figure 1. Granite whole-rock and zircon sample locations superimposed on a gravity image of the Yilgarn Craton, labelled by terrane

at a given FeO_{total}, suggesting that Tibetan granites are generally more oxidized (Fig. 2b). Note that, for samples with FeO_{total} <2 wt%, criteria other than whole-rock Fe_2O_3 and FeO data should be used to assess oxidation state (Blevin, 2004).

Most Yilgarn granites plot in the Cu-infertile field in a V/Sc vs SiO_2 diagram (Fig. 2c; Loucks, 2014), whereas all Tibetan Cu-mineralized granites plot in the Cu-fertile field (Table 1). High V/Sc is caused by amphibole fractionation, which removes Sc, and by suppression of magnetite fractionation, which increases V in an oxidized and hydrous melt (Loucks, 2014). The average V/Sc ratio for each group of Yilgarn granites is significantly lower, suggesting that Yilgarn granites are less fertile than Tibetan granites because the former are generally less oxidized and less hydrous. Zircon saturation temperatures (Watson and Harrison, 1983) indicate that Yilgarn granites crystallized at higher temperatures than Tibetan granites (Fig. 2d), which also suggests they are less hydrous.

The trace element patterns of Yilgarn high Sr/Y and low Sr/Y granites are distinctly different (Fig. 2e). High Sr/Y granites are characterized by an absence of Sr and Eu anomalies, and depletion in heavy rare earth elements (HREE), with an average Yb of about 0.5 ppm. Yilgarn low Sr/Y granites have significant negative Sr and Eu anomalies and elevated HREE concentrations, with an average Yb of about 2 ppm (Table 1; Fig. 2e). These features suggest that Yilgarn high Sr/Y granites were derived from high-pressure melting of mafic crust within the garnet stability field, whereas low Sr/Y granites originated mainly from low-pressure melting of crust within the plagioclase stability field (Moyen and Martin, 2012). Tibetan Cu-mineralized granites have similar HREE patterns to the Yilgarn high Sr/Y granites, but are more enriched in Sr and depleted in Zr (Fig. 2e), consistent with their derivation from high-pressure differentiation of more hydrous melts.

Fertility of Yilgarn granites revealed by zircon compositions

We also compared zircon trace element compositions of Yilgarn granites with those of reference suites of infertile and fertile granites. The zircon REE patterns of Yilgarn granites are similar to both Phanerozoic fertile and infertile suites (Lu et al., 2016), with positive Ce anomalies, negative Eu anomalies, and steep REE patterns with low La/Yb (Fig. 3a). However, Yilgarn granites have consistently lower zircon Ce/Ce* and Eu/Eu* than Phanerozoic fertile suites (Table 2; Fig. 3b,c), suggesting they are less hydrous than fertile suites (Lu et al., 2016).

Zircon Ce/√(U x Ti) was recently proposed as a proxy for magma oxidation state (Loucks and Fiorentini, 2018). Values for Yilgarn granites are lower than those for Phanerozoic fertile suites and similar to those of infertile suites. This also suggests that Yilgarn granites are less oxidized than Cu-fertile granites (Table 2; Fig. 3c), and this is consistent with interpretations from whole-rock Fe_2O_3/FeO data (Fig. 2b).

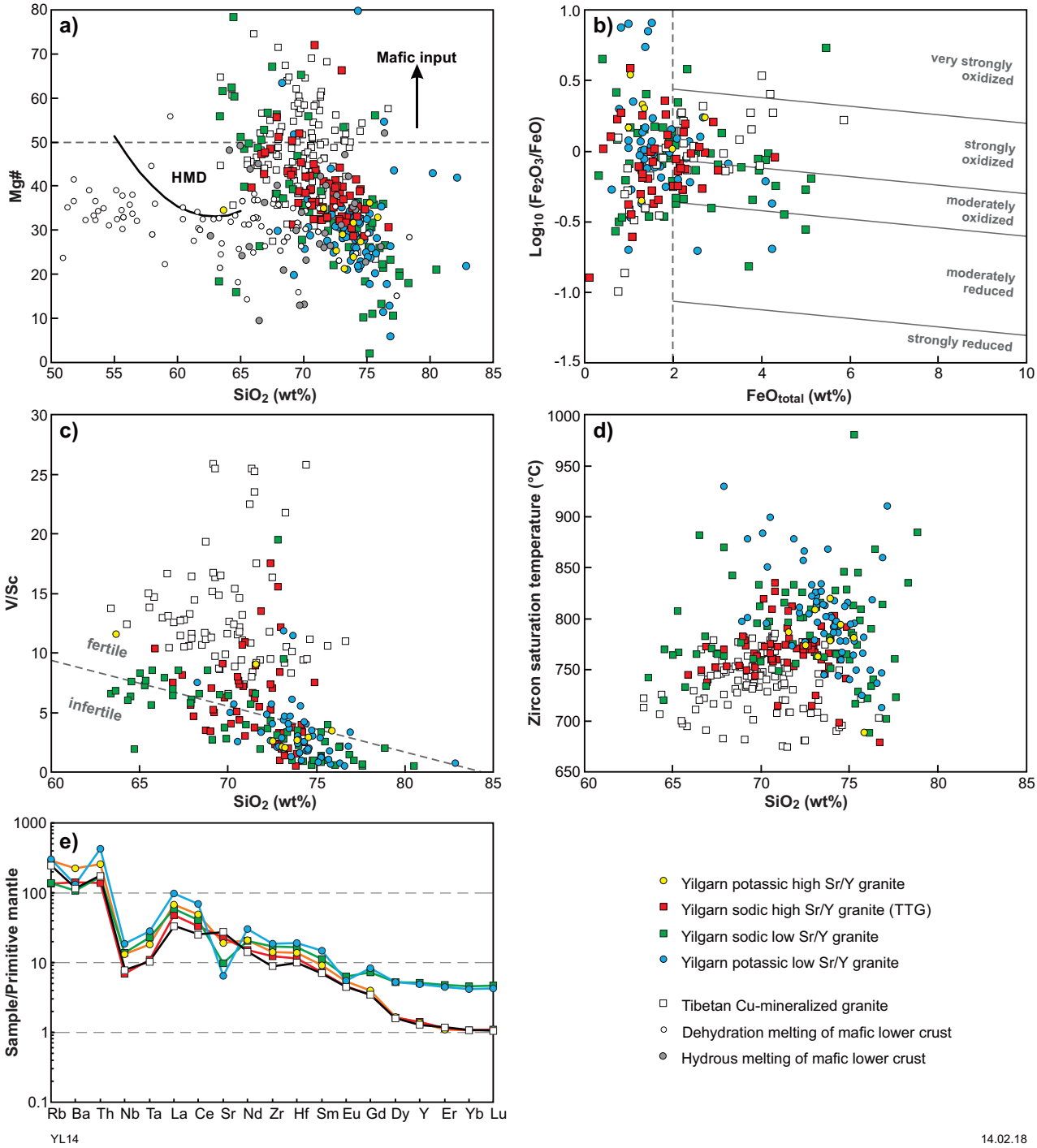

Figure 2. **Whole-rock compositions of Yilgarn granites. Experimental melts from hydrous and dehydration melting of mafic lower crust are plotted for comparison (see Lu et al., 2015 for full references). HMD, high-Mg diorite field, from Lee and Bachmann (2014); Cu-fertile/infertile boundary from Loucks (2014); trace element patterns in e) are normalized to primitive mantle (Sun and McDonough, 1989)**

Table 1. Average compositions of Yilgarn granites and Tibetan Cu-mineralized granites

	Yilgarn potassic high Sr/Y granite		*Yilgarn sodic high Sr/Y granite*		*Yilgarn sodic low Sr/Y granite*		*Yilgarn potassic low Sr/Y granite*		*Tibetan Cu-mineralized granite*	
		sd		*sd*		*sd*		*sd*		*sd*
N	10		65		79		76		117	
Oxides (wt%)										
SiO_2	72.79	3.44	71.50	2.29	71.66	4.37	74.12	2.76	69.78	2.49
TiO_2	0.19	0.06	0.28	0.10	0.35	0.21	0.25	0.13	0.39	0.11
Al_2O_3	14.53	0.98	15.38	0.74	14.32	1.32	13.70	1.16	15.49	1.05
Fe_2O_3T	1.62	0.70	2.09	0.92	2.88	1.57	2.16	1.46	2.46	1.07
MnO	0.03	0.02	0.04	0.03	0.05	0.03	0.03	0.02	0.04	0.02
MgO	0.37	0.23	0.74	0.45	1.07	1.10	0.66	0.95	1.12	0.40
CaO	1.31	0.72	2.33	0.90	2.57	1.92	1.35	1.10	2.29	1.14
Na_2O	3.98	0.61	4.92	0.62	4.59	1.28	3.15	1.10	4.07	0.87
K_2O	5.09	0.86	2.64	1.01	2.42	1.26	4.50	1.07	4.27	1.51
P_2O_5	0.09	0.10	0.09	0.04	0.10	0.07	0.07	0.05	0.14	0.06
Trace elements (ppm)										
Sr	403.0	163.2	480.6	259.5	204.7	122.4	134.7	86.0	579.0	215.7
Zr	155.8	55.9	135.9	42.9	188.1	120.8	207.5	124.4	98.4	29.5
Y	6.2	3.5	6.4	2.9	23.2	28.5	22.4	19.3	5.8	1.7
Yb	0.52	0.29	0.52	0.28	2.23	3.10	2.06	2.03	0.53	0.14
Ratios										
K_2O/Na_2O	1.28	0.13	0.55	0.23	0.56	0.31	2.46	4.42	1.26	1.25
Mg#	29.60	5.14	39.52	7.84	36.16	15.71	30.87	12.10	48.38	9.80
Sr/Y	77.50	36.40	89.80	61.20	14.90	11.30	10.00	9.00	106.40	42.80
La/Yb	114.66	88.74	77.19	56.43	32.02	31.18	52.54	47.26	43.80	13.75
Eu/Eu*	0.96	0.23	0.97	0.20	0.76	0.28	0.56	0.26	0.93	0.12
Nb/Ta	14.07	5.04	14.60	8.38	11.94	4.11	14.05	7.85	13.84	4.01
Dy/Yb	2.43	0.35	2.50	0.82	1.95	0.53	2.10	0.67	2.22	0.33
V/Sc	3.14	4.31	5.88	3.71	4.38	3.33	3.24	2.37	13.59	5.42
T_{zircon} (°C)	777	38	767	27	788	48	803	44	736	27

NOTES: *N*, number of samples averaged; *sd*, standard deviation; T_{zircon}, zircon saturation temperature (Watson and Harrison, 1983). Only samples with LOI <3.5 wt%, SiO_2 >63 wt% and Al_2O_3 <20 wt% are included

Table 2. Average zircon compositions for Yilgarn granites and Phanerozoic reference suites

Granite suite	*N*	*Eu/Eu**	*sd*	*Ce/√(U × Ti)*	*sd*	*Ce/Ce**	*sd*
Yilgarn sodic high Sr/Y granite (TTG)							
Yamarna Terrane	30	0.30	0.08	0.42	0.08	23	15
Burtville Terrane	3	0.41	0.26	0.13	-	5	2
Kalgoorlie–Kurnalpi Terranes	16	0.38	0.17	0.42	0.20	35	19
Murchison Domain, Youanmi Terrane	3	0.42	0.16	0.36	0.07	24	3
Yilgarn sodic low Sr/Y granite	108	0.29	0.09	0.36	0.21	29	35
Yilgarn potassic low Sr/Y granite	41	0.24	0.13	0.34	0.19	49	90
Phanerozoic infertile reference suite	80	0.08	0.07	0.33	0.27	142	215
Phanerozoic fertile reference suite	337	0.59	0.15	0.67	0.39	292	359

NOTES: Phanerozoic reference suites are from Lu et al. (2016). *N*, number of analyses averaged; sd, standard deviation

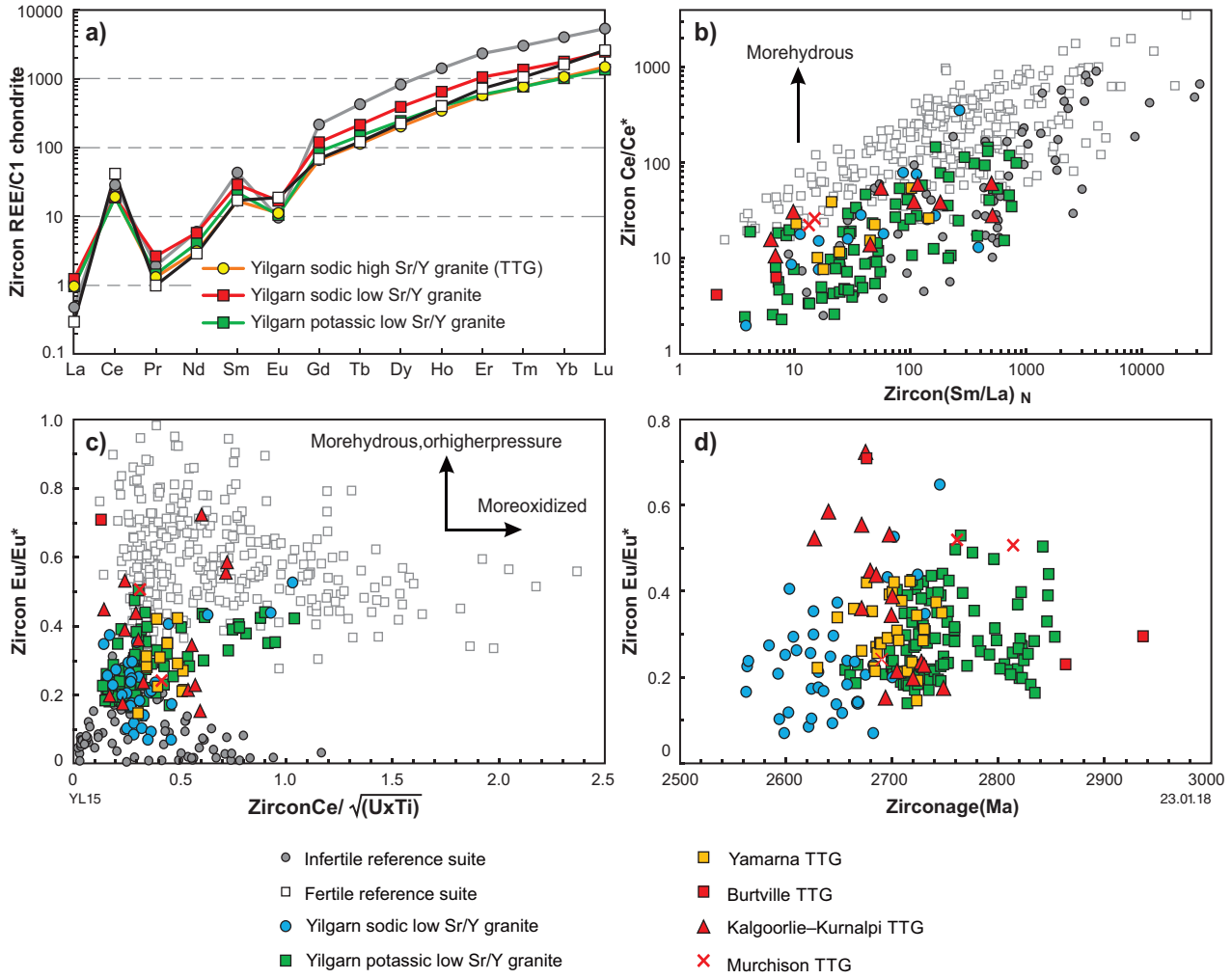

Figure 3. Compositions of zircons from Yilgarn granites. In b), the N subscript indicates values normalized to chondritic values (Sun and McDonough, 1989). Phanerozoic Cu-fertile and Cu-infertile reference suites are from Lu et al. (2016)

Conclusion

Both whole-rock and zircon compositions indicate that many Yilgarn granites are less hydrous and less oxidized than Phanerozoic Cu-mineralized granites. The systematic difference in zircon chemistry between Archean granites and Phanerozoic fertile and infertile suites suggests that different processes were involved in forming Archean granites. We argue that Archean high Sr/Y granites were formed mainly through infracrustal partial melting of mafic lower crust in the garnet stability field, whereas Phanerozoic fertile suites were formed by intracrustal amphibole-dominated fractionation of mafic magmas. Granites formed by the former process have lower potential for porphyry Cu mineralization due to insufficient water and the lack of copper and sulfur accumulation in the melt.

This study employed Yilgarn granite samples currently available in the GSWA database, and did not include granites associated with mineralization. Future work will extend analyses to porphyry-style mineralized Archean granites such as those at Boddington (McCuaig et al., 2001) and at the Calingiri prospect (Outhwaite, 2018). This will assess potential differences between mineralized and non-mineralized Archean granites, and hopefully lead to ways of identifying additional granites that have potential for porphyry-style mineralization.

References

Agnew, P 2015, What industry wants from research: Society of Economic Geologists Annual Conference, World-Class Ore Deposits: Discovery to Recovery, 27–30 September 2015, Hobart, Tasmania, Australia, p. 1–2.

Ballard, JR, Palin, JM and Campbell, IH 2002, Relative oxidation states of magmas inferred from Ce(IV)/Ce(III) in zircon: Application to porphyry copper deposits of northern Chile: Contributions to Mineralogy and Petrology, v. 144, p. 347–364.

Blevin, PL 2004, Redox and compositional parameters for interpreting granitoid metallogeny of eastern Australia: implications for gold-rich ore systems: Resource Geology, v. 54, p. 241–252.

Chiaradia, M, Ulianov, A, Kouzmanov, K and Beate, B 2012, Why large porphyry Cu deposits like high Sr/Y magmas?: Nature, Scientific Reports 2, no. 685, doi:10.1038/srep00685.

Fayol, N and Jebrak, M 2017, Archean sanukitoid gold porphyry deposits: A new understanding and genetic model from the Lac Bachelor gold deposit, Abititi, Canada: Economic Geology, v. 112, p. 1913–1936.

Lee, C-TA and Bachmann, O 2014, How important is the role of crystal fractionation in making intermediate magmas? Insights from Zr and P systematics: Earth and Planetary Science Letters, v. 393, p. 266–274.

Loucks, RR 2014, Distinctive composition of copper-ore-forming arc magmas: Australian Journal of Earth Sciences, v. 61, p. 5–16.

Loucks, RR and Fiorentini, ML 2018, New magmatic oxybarometer using trace elements in zircon reveals oxidation states of Hadean and Eoarchean lithosphere in four cratons: Geochimica et Cosmochimica Acta.

Lu, Y-J, Hou, Z-Q, Yang, Z-M, Parra-Avila, LA, Fiorentini, ML, McCuaig, TC and Loucks, RR 2017, Terrane-scale porphyry Cu fertility in the Lhasa Terrane, southern Tibet, *in* TARGET 2017, Perth, Australia, abstracts *edited by* S Wyche and WK Witt: Geological Survey of Western Australia, Record 2017/6, p. 95–100.

Lu, Y-J, Loucks, RR, Fiorentini, ML, Yang, ZM and Hou, ZQ 2015, Fluid flux melting generated post-collisional high-Sr/Y copper-ore–forming water-rich magmas in Tibet: Geology, v. 43, p. 583–586.

Lu, Y-J, Loucks, RR, Fiorentini, ML, McCuaig, TC, Evans, NJ, Yang, ZM, Hou, ZQ, Kirkland, CL, Parra-Avila, LA and Kobussen, A 2016, Zircon compositions as a pathfinder for porphyry Cu ± Mo ± Au deposits: Society of Economic Geologists Special Publication, v. 19, p. 329–347.

McCuaig, TC, Behn, M, Stein, S, Hagemann, SG, McNaughton, NJ, Cassidy, KF, Champion, DC and Wyborn, LAI 2001, The Boddington gold mine: A new style of Archean Au–Cu deposit, *in* International Archaean Symposium, Extended Abstracts *edited by* KF Cassidy, JM Dunphy and MJ Van Kranendonk: AGSO Record 2001/37, p. 453–455.

McCuaig, TC and Hronsky, JMA 2014, The mineral system concept: The key to exploration targeting: Society of Economic Geologists Special Publication, v. 18, p. 153–175.

Moyen, J-F and Martin, H 2012, Forty years of TTG research: Lithos, v. 148, p. 312–336.

Outhwaite, MD 2018 Metamorphosed Mesoarchean Cu–Mo–Ag mineralization: Evidence from the Calingiri deposits, southwest Yilgarn Craton: Geological Survey of Western Australia, Report 183, 216p.

Sun, S-S and McDonough, WF 1989, Chemical and isotopic systematics of oceanic basalts: implications for mantle compositions and processes, *in* Magmatism in ocean basins *edited by* AD Saunders and MJ Norry: Geological Society of London, Special Publications, v. 42, p. 313–345.

Watson, EB and Harrison, TM 1983, Zircon saturation revisited: Temperature and composition effects in a variety of crustal magma types: Earth and Planetary Science Letters, v. 64, p. 295–304.